Boundary conditions and Natural temperature decay from experimental data analysis to on-design of a tank for CSP plant

Part 2

Alfredo Angelillo[1], Walter Gaggioli[2], Primo Di Ascenzi[2], Valeria Russo[2]

[1] REEFS2–D.Eng., Oslo (Norway)

[2] ENEA–Italian National Agency for New Technologies, Energy and Sustainable Economic Development, Rome (Italy)

Abstract

Translating real boundary conditions in a simulated 2D environment aids to control the performances of a tank prone to store energy. In particular, the ullage has been investigated along a natural decay of temperature since it is a significant observed heat loss along the dome. Whether the tank is prone to store energy along a stand-by phase, during O&M or even in operation, it can affect the performance, maintenance upgrading plans. Experimental data campaigns conducted since 2004 as well as experimental campaigns between 2020 and 2021 have been used to model a lumped-circuit abstraction to focus on heat losses from the upper dome. Those values have been investigated to find a physical law of tank-insulation aging (Angelillo et al., 2021). Under a set of imposed assumptions, a setup of simulation has been used such aid tools to identify a temperature coefficient to visualize the variations of tank performance. Results of data analysis show the characterizing value for tank aging. Therefore, according to a simulated lumped-circuit scheme in OpenModelica in a previous study, has found out key values for more comprehensive energy 2D simulation. Particularly, the lumped-circuit scheme has been used to find the involved thermocouples and translate this accuracy into a temperature coefficient among others. Hence, a set-up of model has been presented to how control it. The novelty of study is based on the opportunity to match a tank design and monitor it along operational phase in no-adiabatic conditions, namely approximately to real conditions.

Keywords: Lumped-circuit, Tank, Storage, O&M

---

1. Introduction

During the experimental campaigns programme SFERA III, at PCS ENEA Casaccia-Rome between 2020 and 2021, has been collected data since 2004 about a series of experiments to study components and the processes of CSP technology (W. Gaggioli et al., 2016). In particular, all those data, both numerical and operating records, haven’t be used to diagnose specific conditions of the system such as errors, shut down, aging, failures and so on. Therefore, the data cataloguing along the campaign has been central to set-up an experiment with the scope to check the performance of some components. The tank SA.1.01 is perfect for the goal because it belongs the experimental power station since 2004 without significant upgrading or updating.

In this regard, heat losses along the natural decay of temperature affect the internal temperatures if the tank set-up lowers the performances in a no-simulated environment, i.e., no adiabatic boundary conditions. Namely, this piece of information could lead to evaluate the state of tank if the original performance has no reached any more, and when.

According to a previous paper (Angelillo et al., 2021) a modelled solution based on lumped-circuit abstraction under a set of imposed assumptions led to a better equation of temperature decay. Regardless of further purposes of the equation, the aim in this paper is to get clear evidence about the aging of tank using the natural decay of temperature. Hence, a time-elapsed comparisons have been done since 2004, even though the paper present only three examples: 2004 first operation year; 2008 after four years of experiments; 2020-2021 the last experimental campaign.

As matter of fact, the natural decay of temperature in the tank is the only condition it can be observed without considering other causes, i.e., increasing parameters and variables.

10.18086/swc.2023.03.01 Available at http://proceedings.ises.org

Furthermore, the immitted energy has shown to exert influence on molten salt level throughout. The two electric flange immersion heaters and the three welded ones along the tank-skin (F. Fabrizi et al., 2006), expand the molten salt while the density reduces (G. Milozzi et al., 2001, K. Cornwell, 1970); to be specific molten salt level varies accordingly. As result, the natural decay, and the level of molten salt inside of the tank are boundary conditions to validate the comparisons of curves, in the absence of significant variations of atmospheric conditions, *ceteris paribus*. To aim to the goal, in accordance with previous paper (Angelillo et al., 2021) of which is an essential part, heat losses have been identified and quantified consistently with the tank geometry and shapes.

The geometry, which has a significant impact (M. Mehos et al., 2020, A.B. Zavoico, 2001), and other implications of data analysis, were explained a previous paper (Angelillo et al., 2021), as such the temperature trends is studied without adiabatic conditions and omission of the tank surface. Other extra information about manipulation of data and measures taken in advance to obtain reliable results has been discussed in the Method paragraph. Subsequently, the paper has focused on the heat loss via ullage, which visualizes the aging of natural temperature decay in SA.1.01 during almost 20 years.

The heat transient has been compared in accordance with a lumped circuit. The fundamentals of heat and mass transfer in relation to the principles of electrostatics, and more generally for what concerns inductances, resistances and capacitors intended also in AC for some configuration, has been used to aid the right modelling of equations. This has led to a novel type of lumped circuit abstraction being applied with time-dependent initial energy for heat transfer. Thereafter some clarifications have been given in the paragraph Methods as well. In fact, the scheme used in the previous paper (Angelillo et al., 2021) has been expanded, showing the parts that were negligible in the case of natural temperature decay. Naturally, such association between the forms of heat transport, both steady-state and thermal transients, are not new in the field, but here the logic finds a new application for the available automation technology.

The heat transient has been compared in accordance with a lumped circuit, Fig. 1; where the fundamentals of heat and mass transfer have been referred to the principles of electrostatics and AC. Those have been used to aid the right modelling of equations. Also, this has led to a novel type of lumped circuit abstraction being applied with time-dependent initial energy for heat transfer. In fact, the scheme used in the previous paper (Angelillo et al., 2021) has been expanded, showing the parts that were negligible at first instance. Naturally, such association between the forms of heat transport, both steady-state and thermal transients, are not new in the field, but here the logic finds a new application for the available automation technology and software like Modelica. Additional clarifications have been given in the next paragraph Methods.

The final purpose by observing the natural decay of temperatures as well as the level trend of molten salts, and stored energy is to optimize the design of all tanks prone to store energy, also to improve Control System during the charging-discharging phase.

2. Method

The manipulation of data recalled the list in Appendix A, have been based on the tagged component changing over time, the several expedients for the experiments, and the DCS images variations. All data have been controlled by operating written PCS records and sorted on the same comparable parameters for the set problem. That is, the molten salt level inside the tank should have been almost the same with a tolerance of ±100 mm in high; no pump motion; no previous pressurization test; all the electric flange and welded heaters switched off; and already at stabilized temperature of molten salt for those were immersed in, and for those corresponding the ullage above.

According to Fig. 1, the resistivity for the convection $\mathbf{h_{ull\text{-}stl}}$ along the interface between the air – ullage – and steel of skin tank has been assumed to have the higher value, namely the same for both horizontal and upwards (Scott M. Flueckinger et al, 2012). The main reason is based on the sheltered area where the tank is located. This area could easy been assumed to have the same outdoor temperature downwards, horizontal, and upward, hence the same for the free stream condition resistance $\mathbf{R_{\infty}}$. That is, the heat flow has almost the same ΔT along the ullage. Precisely, the outdoor temperature has matter if we reach lower temperature after freezing phase (W. Gaggioli et al., 2017), or where the oscillations among days and nights could be significant at lower temperature. Generally, outdoor temperature at PCS location in Rome can be assumed as temperature mean of day, i.e., no meaningful diurnal air temperature variation. As consequence, the insulation resistance $\mathbf{R_{iso}}$ from the ullage plus the interface $\mathbf{h_{ull\text{-}stl}}$ is the same along the whole ullage volume.

The molten salt dome followed the same logic downwards, that is to use the higher convection $\mathbf{h_{ms\text{-}stl}}$. In this case, the horizontal one is the higher value than downwards one. As matter of fact, the paper (Angelillo et al., 2021) held about a reliable way to find out a superficial outer tank temperature without having any measurement on the outer skin-tank along the collected data. Thus, obtaining an expression entirely dependent on physical and geometric parameters. Furthermore, the skin-temperature could be intended as quasi-uniform, but the proportion between the molten salt mass and ullage becomes fundamental, both to assume it, and how to determine those temperatures.

$$T_0(\tau, H_{lms}) = \sum\left(\left(\prod_i \frac{T_{TT,max,i}+T_{TT,min,i}}{2}\,\frac{V_{ms,i}}{V_T}\right)^{\frac{1}{i}} + \left(\prod_j \frac{T_{TT,max,j}+T_{TT,min,j}}{2}\,\frac{V_{ull,j}}{V_T}\right)^{\frac{1}{j}}\right)_{,k} \frac{\Delta\tau_k}{\Delta\tau} \qquad \text{(eq.1)}$$

Hence, $T_0(\tau, H_{lms})$ is the initial temperature weighted as a function of the time intervals in which the salt level and the volume of the salts vary. Assumed that, the subscripts $_{\mathbf{ull}}$ refer to ullage, and $_{\mathbf{ms}}$ refer to molten salt volume underneath, the initial temperature depends on the level of molten salt or likewise the ullage above, so the initial skin temperature increases with bigger molten salt volume or decreases with the bigger ullage ones according to the transient. This is the start point for the natural decay of temperatures. Trivially, where the molten salt volume $V_{ms} = 0$, i.e., no molten salt in the tank, the formula calculates the skin-temperature by only the air inside the tank.

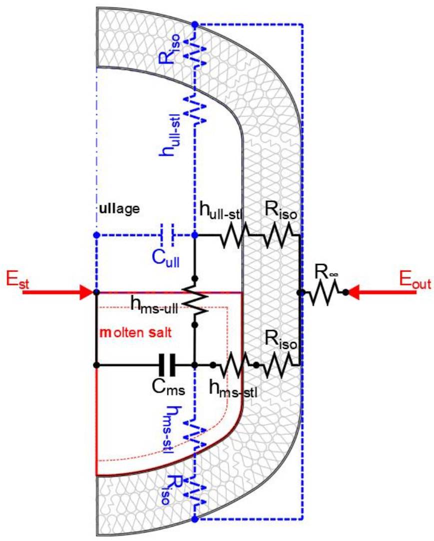

Fig. 1 Extended lumped circuit in use for modelling equation and simulations. The blu dashed lines are the negligible values in consistency with boundary conditions.

On the reporting of the experimental campaigns and historical data, the most consistent way to test statements and assertions is to use the variations between those two volumes in comparable volumes as well as minimizing significant pressure variation. On purpose, the decay temperature trends are based on ullage around 52%.

In accordance with extended lumped circuit in Fig. 1, the ullage capacitor $\mathbf{C_{ull}}$ was neglected in (Angelillo et al., 2021) due to a scale factor between air and molten salts. Indeed, the pressure inside the tank is assumed and it is almost constant, realistically. That is all the physics phenomena are at constant pressure. If so, we can consider taking the variations of the physical parameters of the air at constant pressure. That means two parallel connected capacitors are the sum of capacitors, but where the $\mathbf{C_{ull} \ll C_{ms} : \{C_{ull}+C_{ms}\} \approx C_{ms}}$. Although, it is considered that the heat from the molten salts subsequently releases to the ullage via the interface $\mathbf{h_{ull\text{-}stl}}$ will be a small negligible amount of energy that the air can store.

So, assumed that: $\begin{cases} C_{ms} = c_{p,ms} m_{ms} \\ C_{ull} = c_{p,air} m_{air} \end{cases}$ (eq.2)

in accordance with thermal-physical properties and constitutive correlation, Appendix B, the capacitor $\boldsymbol{C_{ull}}$ is around 0,04% of total amount of loaded energy, simply negligible. As matter of fact, the air has no resilience in accordance with material science. Methodologically, the attention was set on the heat flow and the velocity of heat losses via ullage to define the boundary conditions into the simulated environment.

Firstly, the domes have longer characteristic length that result into a worse form factor and act as disperser. The factor forms for the cylindrical part of PCS SA.1.01 is 2,02 m^{-1}, while only the dome is almost 9,45 m^{-1}. This result stand for 45% of total heat loss by domes. Naturally, the upwards dome is worse than the downwards one. The first is interfaced with air, while the downwards contains molten salts with significant higher specific heat at constant pressure.

Secondly, the interface $\mathbf{h_{ull\text{-}st}}$, as mentioned above, is based on a lower resistivity and higher velocity. Based on the recorded temperature inside the tank and on the skin steel under the isolation layer, that could be guessed, this convection heat transfer coefficient at boundary layer $\boldsymbol{y} = 0$ is (T.L. Bergman et al., 2017):

$$h_{ull-stl} = \frac{-\lambda_{air}(T)\frac{\partial T}{\partial y}\Big|_{y=0}}{T_s - T_{\infty,ull}} \quad \text{(eq.3)}$$

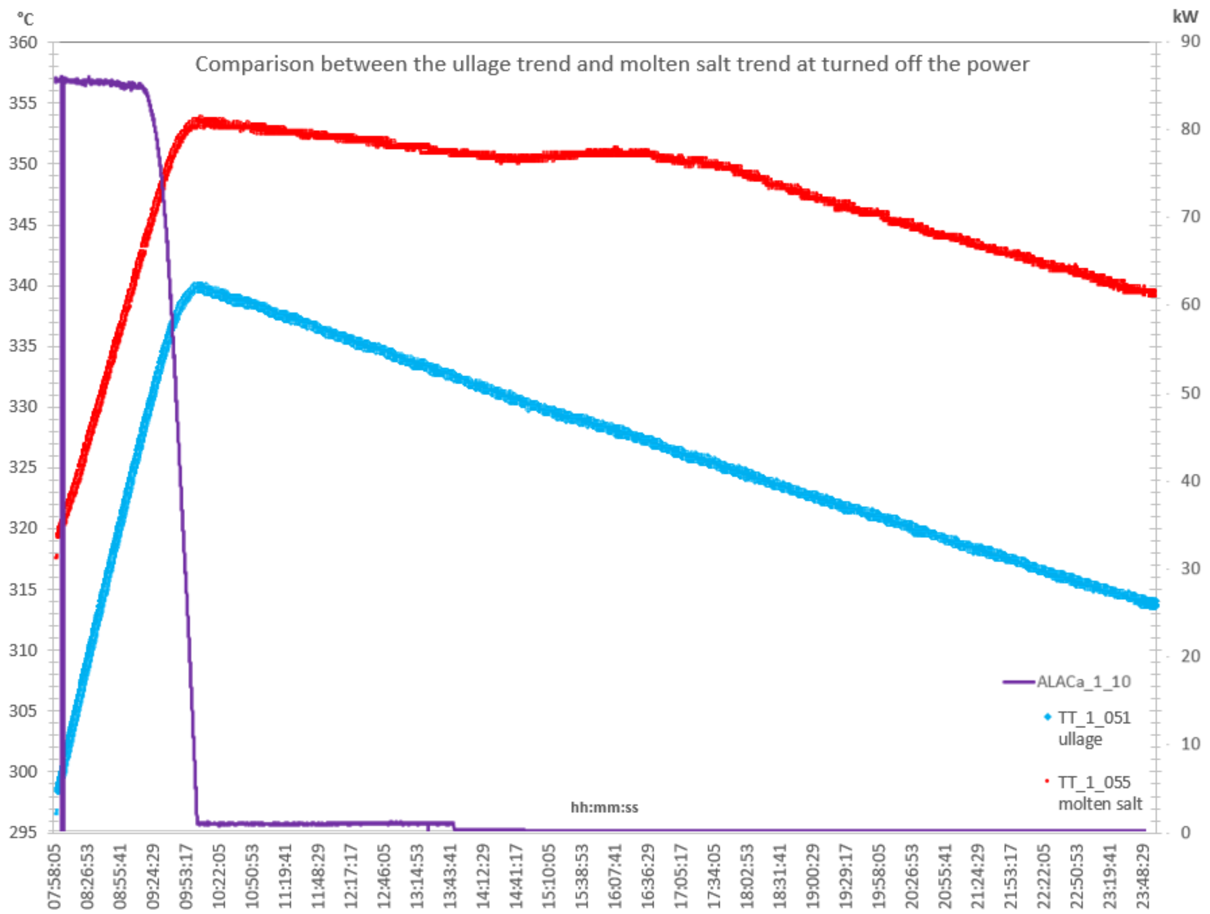

Fig. 2 The immersed thermocouple in molten salt (red line) and in ullage (blue line) compared to power (violet line)

As the distance $\boldsymbol{y}$ between the inner side of tank surface and centre of ullage increases, so the velocity must be consistent to the variations of time related to the variation of temperatures on the surface, that is:

$$\tau_{ull} = \mu(T) \frac{\partial u}{\partial y}\Big|_{y=0} \quad \text{(eq.4)}$$

The upwards convection transfer coefficient is the one used inside the ullage despite of directions, because the historical trends of air inside the tank have shown a precise curve in comparison to the molten salt; namely an immediate higher heat loss according to downwards convexity of the thermocouple trend, Fig. 2.

This figure (Fig. 2) visualizes the beginning of temperature natural decay where the switched off power sets the trend of ullage temperature to decrease quasi-immediate. That has been verified to match a capacity for air mass around 727 J°C^{-1}m^{-3} *versus* a 47% molten salt mass of the total tank volume, ca. 2,63 MJ°C^{-1}m^{-3}. Therefore, it can be assumed that the ullage heat loss reaches own energy level immediately, and right after it dropped down in comparison to the resilience of molten salt mass, i.e., the first part of red line at switched off power in Fig. 2. The molten salt takes almost 8 hours to reach the decay point inertially, while the ullage has doubled the ΔT in comparison to molten salt trend after 4 hours. Conclusively, in this way the methodology has taken into account the strong correlation between molten salt level, temperature, stored energy and physics parameters.

3. Results

The analysis of data listed in Appendix A has led to identify a way to signal aging, namely the performance of the tank after 17 operating years. The trends in Fig. 3 and Fig. 4 show the comparisons of the curves in the three referenced mentioned years: 2004 first operation year; 2008 after four years of experiments; 2020-2021 the last experimental campaign. In accordance with methodology and the parameters used to evaluate the transient of natural temperature decay, and collected data with same weather conditions, it was avoiding significant swings in temperatures during the long necessary time to reach the freezing point of molten salt volume. Consequentially, the comparisons are based on the same outdoor temperature mean between 10°C and 15°C.

The reference year is 2004, the first operational year for PCS, depicted with orange line in both Fig. 3 and Fig. 4. The mentioned period in 2004 is between 6th and 10th of April with outdoor temperature mean of 12,48°C and ±2,42°C diurnal air temperature variation. The level of molten salt during the same period in NO-operational or stand-by mode conditions was between 1171 mm and 1235 mm within the predetermined ±100 mm tolerance range. The thermocouple TT_1_051 is the highest one installed on SA.1.01 tank and measured the ullage without been affected by other causes. Furthermore, the operational records aided to recognize activity that could have invalidated the result. In Fig. 4 the trend of TT_1_051 shows the most suitable period among the 5 days data, while in Fig. 3 is the same, but shorter in comparison to 2008's data trend. In particular, before beginning of natural decay in 2004, Fig. 4, the trend is affected by two electric flange immersion heaters to reach the set point 320°C, and at the end the power was switched on to hold the molten salt over the freezing point, i.e., around 260°C. Between these two moments, it was recorded a natural decay of temperatures, used here as representative specimen of the recorded data in 2004.

The first comparison is along the 12th of March 2008 between 9:05 and 17:40 o'clock, blue marker in Fig. 3. The outdoor temperature mean was 13,1°C and ±2,9°C diurnal air temperature variation. The referred level of molten salt was 1086 mm and 1114 mm with a deviation of 8,46% compared with the referenced curve. The operational records in 2008 aided to interpret the trend of curve correctly. That date was planned a reparation on central siphon, so the solar field was switched off, hence the natural decay of temperature took place until a pump was reactivated again as shown into Fig. 3. For the comparison, the natural decay in the diagram is settled in the same period of time and temperature difference, thereby it is seen another tangential variation between the two mentioned years.

The second comparison refers to the experimental campaign between 17th and 25th of October 2020, the grey line in Fig. 4. The experimental set-up was to collect data from the tank SA.1.01 after reaching the set-point of 500°C and leave temperature to decay to 300°C, the most common period observed since 2004. The outdoor temperature mean along the week was 15,1°C and ±5,1°C diurnal air temperature variation with a deviation around 9,07%. To avoid significant diurnal air temperature variation, the comparison focused on the daylight part of data, even though it has been confirmed in a time-elapsed observation each 4 years along different days, *ceteris paribus*. As matter of fact, some deviations have been observed with decreasing outdoor temperatures, see Fig. 4, even though a same tangential angle of the curve is in place. As expected, the natural decay in the same period of time, x-axis, and the temperature difference, y-axes, had an even worse inclination in comparison to the ones in 2004, also bigger than 2008 as in Fig. 3 and Fig. 4.

These comparisons have given evidence to pursue that the tank had lowering performances along the years. As result, it is self-evident that the insulation layer is reducing its performance capabilities along its lifespan since the layers in place for 17 years have been the steel tank, the insulation, and the aluminium cladding, and considered that the metal layers have not shown sign of corrosion or deterioration.

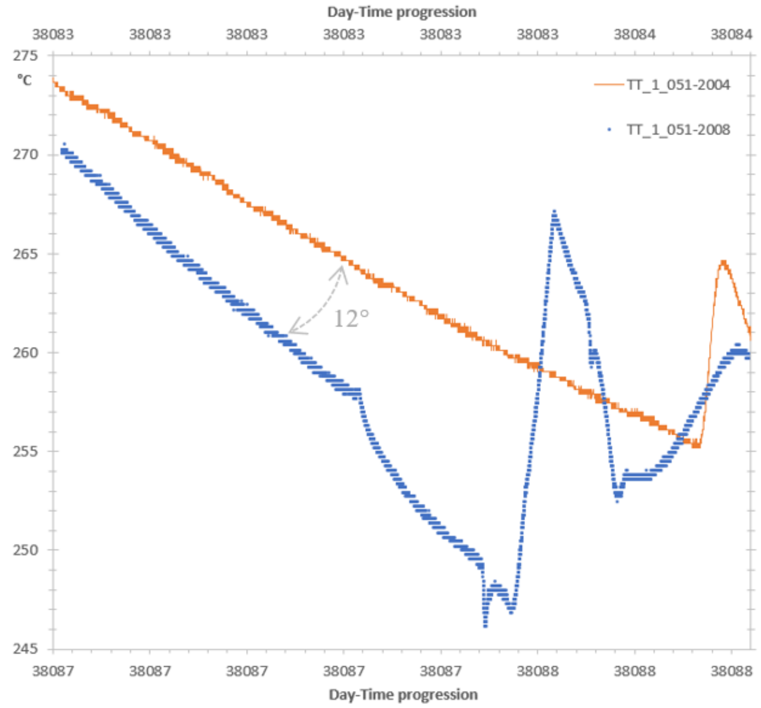

Fig. 3 Comparison between the same thermocouple in two different years, 2004 in orange and 2008 in blue. The curves have a tangential variation of 12°.

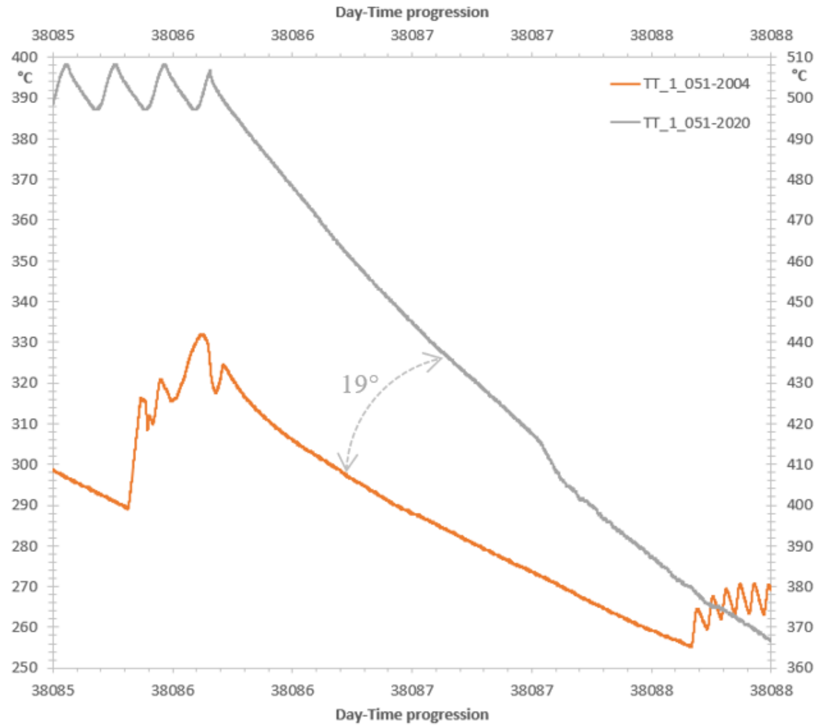

Fig. 4 Comparison between the same thermocouple in two different years, 2004 in orange and 2020 in grey. The curves have a tangential variation of 19°.

4. Simulation Set-up

In this paper, only the simulations that have an interest in terms of thermal losses and the verification of the hypotheses made in non-adiabatic conditions are taken into consideration. In particular, the aim was to verify a modelling of the tank with a set-up of parameters that are consistent with the experimental tests as well as to verify and control the heat loss areas. The same model has used for further insights that will be developed in subsequent papers.

The physical characteristics of the materials in use are indicated in Appendix B, which have been applied in the temperature range 260°C – 500°C. In accordance with the assumptions made in paragraph Method, the steel shell is not taken into consideration, nor is the external radiosity solver, to reduce the need for negligeable calculations.

The simulation area is 2,5*4,0 meters, divided into 4 shaped elements: external environment, molten salts, ullage, and insulation. The boundary conditions of the simulation area are set as Neumann condition, constant heat flux equal to 0°Cm^{-1}. In addition, a condition is set on the vertical plane to the screen to obtain a better performance of the diffusivity step of the Navier-Stockes equations. The focus is on speed, i.e., advection step in the governing equations, to verify the correspondence between the horizontal losses along the tank-wall and those vertical along the ullage as investigated.

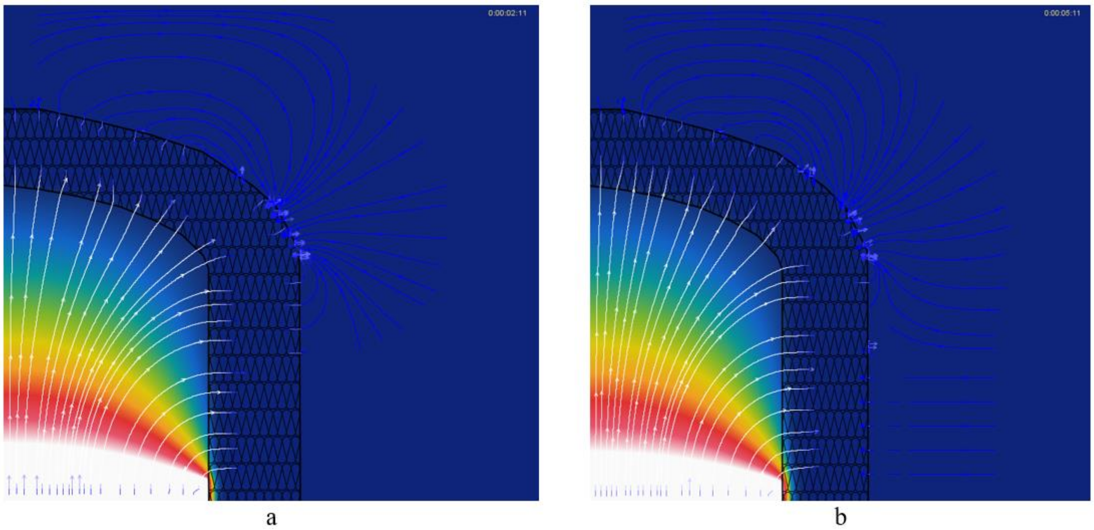

Fig. 5 Simulation in free stream convection conditions for outdoor temperatures and ullage dome.

Specifically, since the external temperature is much lower, it has been modelled as a shaped block around the tank with the physical parameters of the air at the average temperature of 12,5°C. This has made it possible to obtain a certain simplification of the calculation without losing results for the heat flux lines. In fact, Fig. 5 a and b show the heat flux lines in the case of free stream convection simulation of ullage side model, where the heat flux lines intersect at a distance similar to the tangents of the iso-heat flux lines in Fig. 6. This allows to consider negligible the body force such as gravity or buoyancy into Navier-Stockes equation **f**, in some circumstances, or indeed to take it as a negligible constant according to air parameter at outdoor temperature. As matter of fact, assumed that the reference Navier-Stock equation is,

$$\frac{\partial \mathrm{v}}{\partial \tau} = \alpha \nabla^2 \mathrm{v} - (\mathrm{v} \cdot \nabla)\mathrm{v} - \nabla p + f, \qquad \text{(eq.5)}$$

the Fig. 5 visualizes the outdoor air in free stream convection condition, dissimilar to Fig. 6 where the outdoor air is modelled as an element with an initial temperature of 12,5°C Fig. 5. The difference lies in the divergence of the part of the Navier-Stockes equations dependent on the advection step which can cause instability especially with increasing external wind speed. However, the set boundary conditions avoid that calculations blow up. Since the tank is placed in a totally sheltered area, this allows to observe no blow up simulation occurred with a very short time step length, but that the heat loss towards the dome of the ullage, Fig. 5a, occurs before the horizontal one of the tank wall, Fig. 5b. The heat flux lines are affected by the absence of diffusivity in the plane orthogonal to the screen of the 2D simulation to increase the advection component in the Navier-Stockes equations. Furthermore, the variation between the boundary conditions for Fig. 5 compared to Fig. 6 do not give significant variations in the output of the heat flux lines, with the exception of the Neumann boundary conditions of simulation area which enclose all the heat flux lines.

Consistent with the data analysed, the simulations Fig. 6 were performed in the aforementioned temperature range corresponding to a constant density, kinematic and dynamic viscosity of the two mediums, varying the properties of the air tank temperatures lower than approximately 226 °C that is, up to an external air temperature of 12,5°C according to measured value. The error for the constant molten salt density along the temperatures mentioned, such as reported in the simulations, has been measured equal to 1,1%.

The simulation of the natural decay of molten salt temperatures, Fig. 6, has a power source with a set-point from 300°C to 260°C. Setting a temperature coefficient of -0,5°C, i.e., it is in agreement to an increase in the decay rate equal to about three times that one actually occurred, considering a step length of 0,025 seconds in comparison to 0,0004°Cs^{-1} detected by experimental data for the reference year 2004.

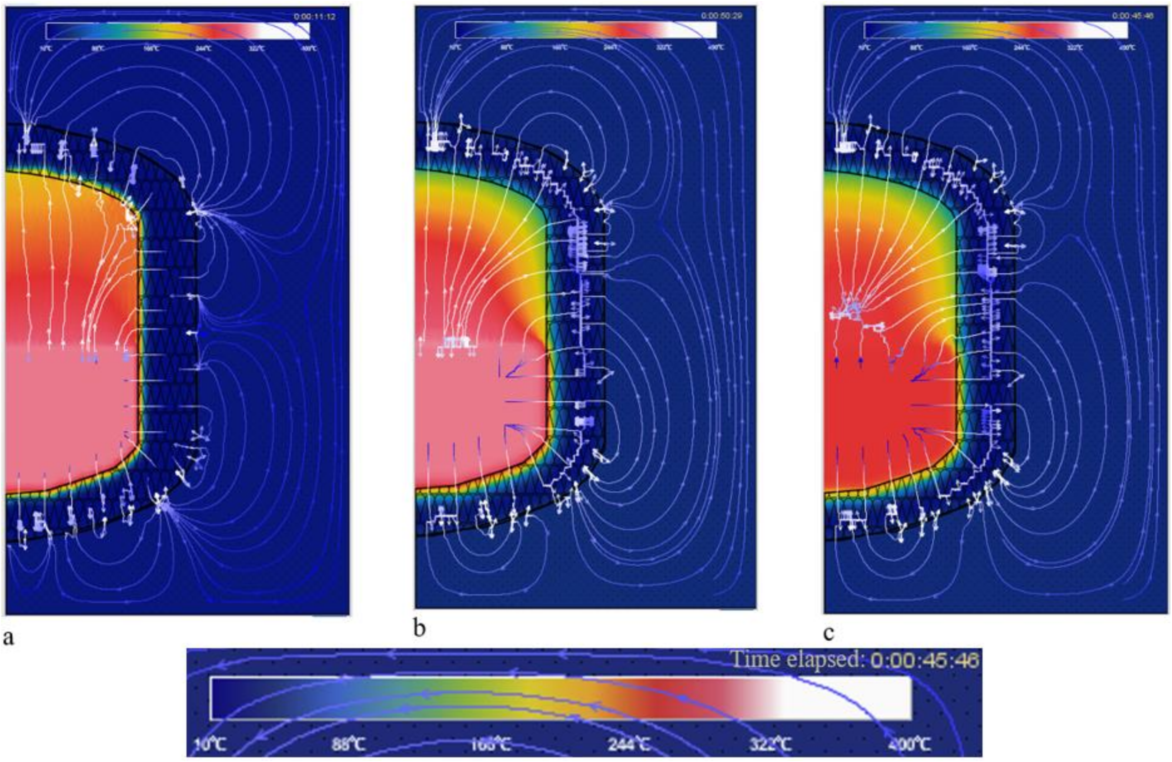

Fig. 6 Simulation in free stream condition inside the ullage with initial outdoor temperature of 12,5°C.

5. Conclusions and Outlook

The transient of temperature decay data could lead to a novel method to control operational and maintenance conditions or to improve the design. This paper has reinforced previous paper (Angelillo et al., 2021) of which is an essential part. Particularly, the heat losses via ullage are of fundamental importance for the analysis of temperature decay because air is lack of resilience capability and has a significantly lower specific heat in comparison to molten salt. Besides the ullage and molten salt volumes mutually influence temperatures and heat losses flow through the tank. To be precise, the ullage has presented a more suitable ability to be compared since the heat, close to the inner tank, becomes conductive without any other causes.

As matter of fact, the lumped-circuit abstraction and 2D visual simulations has been a support to investigate and evaluate key-parameters, such as superficial temperature which are crucial of calculating heat flow. Several simulations have been carried out to set up a reliable model to identify the key parameters with the aim of comparing variations of performance. While the physical parameters could be held constant throughout the lifespan, a temperature coefficient consistent with natural decay of temperatures can be crucial to identify the aging.

Accordingly, the geometry of tank has also been discussed in compliance of the lumped circuit, i.e., electrical capabilities of suited components. In addition to this, the velocity of heat loss from the ullage has been analysed related between convection, temperature, and immediate conduction towards the outer layer. As result, the recorded data of ullage, which depict the heat loss from the inner to the outer side of the tank according to boundary conditions in force, can be compared to evaluate in which size an insulation layer is still capable of performing correctly. To do so, the data over the years must be admissible and comparable. Admissible stands for to be inside a percentage of deviations it doesn't alter results. Comparable means to be defined as equivalent or that can be approximate confidently.

An outlook of lumped-circuit, i.e., the mention Modelica simulation and 2D energy simulation, the variation of the ullage-air in regard to increase or decrease the mass of salts with the heat flow in no-adiabatic conditions will be part of more comprehensive paper.

Finally, this novel study can be used to evaluate the condition in operation of a tank whichever a storage or prone to it, but also it could orient to introduce a new perspective in a project phase in terms of design and quantity of molten salt as storage.

Acknowledgement

We thank ENEA for the support of its scientific and technical staff provided during the accesses SURPF2001170003A and SURPF2201170005 to PCS facility. The access SURPF2001170003A was arranged in the frame of H2020 SFERA-III project activities – European Union's Horizon 2020 G.A. n. 823802 –.

References

A. Angelillo, W. Gaggioli, P. Di Ascenzi, Boundary conditions and Natural temperature decay from experimental data analysis to on-design of a tank for CSP plant – Part 1, ISES Conference Proceedings (2021) Solar World Congress

A.B. Zavoico, Solar power tower design basis document. Sandia National Laboratories. Report no. SAND2001-2100

F. Fabrizi, W. Gaggioli, L. Rinaldi, P. Tarquini, Applicazioni della tecnologia solare termodinamica sviluppata dall'ENEA in impianti di piccola taglia per la produzione di energia elettrica e termica in processi industriali e civili, ATI, 2006

K. Cornwell, The thermal conductivity of molten salts, Department of Mechanical Engineering, Edinburgh, 1970

Mehos, Mark, Hank Price, Robert Cable, David Kearney, Bruce Kelly, Gregory Kolb, and Frederick Morse, Concentrating Solar Power Best Practices Study, Golden, CO: National Renewable Energy Laboratory. NREL/TP-5500-75763, 2020

Miliozzi, G.M. Giannuzzi, P. Tarquini, A. La Barbera, Fluido termovettore: dati di base della miscela di nitrati di sodio e potassio, s.l. 2001 – Doc.ENEA/SOL/RS/2001/07

Scott M. Flueckiger, Suresh V. Garimella, Second-law analysis of molten-salt thermal energy storage in thermoclines, Solar Energy, 86 (2012): 1621-1631

T. L. Bergman, A. S. Lavine, Fundamentals of heat and mass transfer, Wiley, 8th edition 2017

W. Gaggioli, F. Fabrizi, L. Rinaldi, P. Di Ascenzi, Experimental tests about the cooling/freezing of the molten salts in the receiver tubes of a solar power plant with parabolic trough conditions, AIP Conference Proceedings 1850, (2017) 020005.

W. Gaggioli, P. Di Ascenzi, L. Rinaldi, P. Tarquini, F. Fabrizi, Effects assessment of 10 functioning years on the main components of the molten salt PCS experimental facility of ENEA, AIP Conference Proceedings 1734, (2016) 070009

Appendix A

Tab. 1 ENEA experimental data, received and analyzed, in accordance with the PCS operating conditions ongoing recorded on log-book between 2004 and 2022.

Prg.	Date in:	Prg.	Date in:	Prg.	Date in:
1	02.04.2004	14	20.05 to 22.05.2004	27	30.07 to 31.07.2005
2	05.04 to 08.04.2004	15	25.06 to 23.08.2004	28	23.09 to 26.09.2005
3	09.04 to 12.04.2004	16	24.08 to 27.08.2004	29	25.11 to 28.11.2005
4	13.04 to 16.04.2004	17	28.08 to 29.08.2004	30	28.02.2008
5	17.04 to 19.04.2004	18	30.08 to 31.08.2004	31	12.03.2008
6	20.04 to 21.04.2004	19	01.09 to 17.09.2004	32	01.04.2008
7	26.04 to 30.04.2004	20	14.01 to 18.01.2005	33	03.04 to 07.04.2008
8	01.05 to 02.05.2004	21	04.02.2005	34	03.04 to 07.04.2008
9	07.05.2004	22	10.02.2005	35	30.05 to 03.06.2008
10	14.05.2004	23	17.02 to 21.02.2005	36	09.07.2008
11	17.05.2004	24	06.04.2005	37	01.10.2008
12	18.05.2004	25	13.05.2005	38	17.10.2008
13	19.05.2004	26	15.07 to 19.07.2005	39	25.10.2008
40	31.10 to 04.11.2008	45	08.05 to 12.05.2012	50	05.09 to 06.09.2018
41	28.11 to 30.11.2008	46	09.06 to 25.06.2012	51	17.09 to 18.09.2018
42	01.12.2008	47	13.07.2012	52	17.10 to 25.10.2020
43	16.12.2008	48	08.12 to 12.12.2016	53	03.02 to 04.02.2021
44	22.11 to 28.11.2008	49	27.08 to 30.08.2018	54	20.07 to 15.09.2021

Appendix B

Tab. 2 Thermal-physical properties and constitutive correlation to the temperature

Material	Thermal physical property	Equation
Air, *air = ull*	Thermal conductivity, k_{air}	$k_{air} = 0{,}224 + (8{,}02)10^{-4}\,T - (3{,}28)10^{-7}\,T^2 [W\,m^{-1}\,°C^{-1}]$
	Density, ρ_{air}	$\rho_{air} = 2{,}8953 + 0{,}26733\,T + 132{,}45\,T^2 + 0{,}27341\,T^3 [K]\,[kg\,m^{-3}]$
	Specific heat, $c_{p,air}$	$c_{p,air} = 0{,}10 + (1{,}40)10^{-4}\,T + (1{,}01)10^{-7}\,T^2 - (5{,}69)\,10^{-11}\,T^3\,[J\,kg^{-1}°C^{-1}]$
	Viscosity, μ_{air}	$\mu_{air} = [0{,}1726 + (4{,}52)10^{-4}\,T - (1{,}937)10^{-7}\,T^2 + (4{,}185)10^{-11}\,T^3]\,10^{-4}\,[°C]\,[kg\,m^{-1}s^{-1}]$
Stone mineral wool,*iso*	Thermal conductivity, k_{iso}	$k_{iso} = 0{,}106\,[W\,m^{-1}\,K^{-1}]$

	Density, ρ_{iso}	$\rho_{iso} = 100[kg\ m^{-3}]$
	Specific heat, $c_{p,iso}$	$c_{p,iso} = 1030\ [J\ kg^{-1}K^{-1}]$
Molten salt, *ms*	Thermal conductivity, k_{ms}	$k_{ms} = 0{,}443 + 1{,}9 \times 10^{-4}\ T\ [W\ m^{-1}\ °C^{-1}]$
	Density, ρ_{ms}	$\rho_{ms} = 2090 - 0{,}636\ T[°C]\ [kg\ m^{-3}]$
	Specific heat, $c_{p,ms}$	$c_{p,ms} = 1443 - 0{,}172\ T\ [J\ kg^{-1}°C^{-1}]$
	Viscosity, μ_{ms}	$\mu_{ms} = [22{,}714 - 0{,}12\ T + 2{,}281 \times 10^{-4}\ T^2 - 1{,}474\ \times 10^{-7}\ T^3]\ \times 10^{-3}[°C]\ [kg\ m^{-1}s^{-1}]$
Steel, *stl*	Thermal conductivity, k_{stl}	$k_{ms} = 60\ [W\ m^{-1}\ K^{-1}]$
	Density, ρ_{ms}	$\rho_{stl} = 8000[kg\ m^{-3}]$
	Specific heat, $c_{p,stl}$	$c_{p,stl} = 480\ [J\ kg^{-1}K^{-1}]$
Aluminum, *alu*	Hemispherical emissivity	$\varepsilon = 0{,}1\ [-]$

Appendix C

Tab. 3 Acronyms

Acronyms	**Explicit**
ENEA	Energia Nucleare ed Energie Alternative = Nuclear Energy and Alternative Energy
O&M	Operating and Maintenance
PCS	(stazione di) Prova Collettori Solari = Solar Collector Test (station)
CSP	Concentration Solar Power
AC	Alternating Current
DCS	Distributed Control System